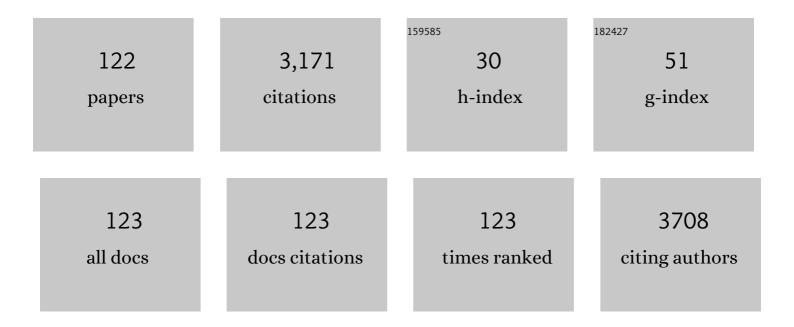
List of Publications by Year in descending order

Source: https://exaly.com/author-pdf/3501582/publications.pdf Version: 2024-02-01



LE ZUENC

#	Article	IF	CITATIONS
1	Airway Remodeling Measured by Multidetector CT Is Increased in Severe Asthma and Correlates With Pathology. Chest, 2008, 134, 1183-1191.	0.8	260
2	3D MRI-Based Multicomponent FSI Models for Atherosclerotic Plaques. Annals of Biomedical Engineering, 2004, 32, 947-960.	2.5	196
3	Coronary Arteries: Magnetization-prepared Contrast-enhanced Three-dimensional Volume-targeted Breath-hold MR Angiography. Radiology, 2001, 219, 270-277.	7.3	119
4	Quantifying Effects of Plaque Structure and Material Properties on Stress Distributions in Human Atherosclerotic Plaques Using 3D FSI Models. Journal of Biomechanical Engineering, 2005, 127, 1185-1194.	1.3	114
5	Effect of Stenosis Asymmetry on Blood Flow and Artery Compression: A Three-Dimensional Fluid-Structure Interaction Model. Annals of Biomedical Engineering, 2003, 31, 1182-1193.	2.5	111
6	Local Maximal Stress Hypothesis and Computational Plaque Vulnerability Index for Atherosclerotic Plaque Assessment. Annals of Biomedical Engineering, 2005, 33, 1789-1801.	2.5	108
7	Concurrent multimodality image segmentation by active contours for radiotherapy treatment	3.0	107
8	Right and Left Ventricular Myocardial Perfusion Reserves Correlate with Right Ventricular Function and Pulmonary Hemodynamics in Patients with Pulmonary Arterial Hypertension. Radiology, 2011, 258, 119-127.	7.3	107
9	Contrast-enhanced MR Imaging of Coronary Arteries: Comparison of Intra- and Extravascular Contrast Agents in Swine. Radiology, 2001, 218, 670-678.	7.3	73
10	Across all solid organs, adolescent age recipients have worse transplant organ survival than younger age children: A <scp>US</scp> national registry analysis. Pediatric Transplantation, 2015, 19, 471-476.	1.0	62
11	Image-based modeling for better understanding and assessment of atherosclerotic plaque progression and vulnerability: Data, modeling, validation, uncertainty and predictions. Journal of Biomechanics, 2014, 47, 834-846.	2.1	59
12	Effects of cognitive training with and without aerobic exercise on cognitively demanding everyday activities Psychology and Aging, 2014, 29, 717-730.	1.6	58
13	Gadocoletic Acid Trisodium Salt (B22956/1). Investigative Radiology, 2006, 41, 279-291.	6.2	48
14	Cytokine response after severe respiratory syncytial virus bronchiolitis in early life. Journal of Allergy and Clinical Immunology, 2008, 122, 726-733.e3.	2.9	43
15	Assessment of regional differences in myocardial blood flow usingT2-weighted 3D BOLD imaging. Magnetic Resonance in Medicine, 2001, 46, 573-578.	3.0	42
16	Quantitative and Semiquantitative Measures of Regional Pulmonary Microvascular Perfusion by Magnetic Resonance Imaging and Their Relationships to Global Lung Perfusion and Lung Diffusing Capacity. Investigative Radiology, 2013, 48, 223-230.	6.2	42
17	PET/MRI of Hypoxic Atherosclerosis Using <sup>64</sup> Cu-ATSM in a Rabbit Model. Journal of Nuclear Medicine, 2016, 57, 2006-2011.	5.0	41
18	Accurate myocardialT1 measurements: Toward quantification of myocardial blood flow with arterial spin labeling. Magnetic Resonance in Medicine, 2005, 53, 1135-1142.	3.0	40

#	Article	IF	CITATIONS
19	Longitudinal Changes in Airway Remodeling and Air Trapping in Severe Asthma. Academic Radiology, 2014, 21, 986-993.	2.5	40
20	Three-Dimensional Gadolinium-Enhanced Coronary Magnetic Resonance Angiography: Initial Experience. Journal of Cardiovascular Magnetic Resonance, 1999, 1, 33-41.	3.3	38
21	Lack of significant improvements in longâ€term allograft survival in pediatric solid organ transplantation: A <scp>US</scp> national registry analysis. Pediatric Transplantation, 2015, 19, 477-483.	1.0	38
22	Fast mapping of myocardial blood flow with MR firstâ€pass perfusion imaging. Magnetic Resonance in Medicine, 2008, 59, 1394-1400.	3.0	37
23	Combined MR proton lung perfusion/angiography and helium ventilation: Potential for detecting pulmonary emboli and ventilation defects. Magnetic Resonance in Medicine, 2002, 47, 433-438.	3.0	36
24	The quantification of blood-brain barrier disruption using dynamic contrast-enhanced magnetic resonance imaging in aging rhesus monkeys with spontaneous type 2 diabetes mellitus. NeuroImage, 2017, 158, 480-487.	4.2	36
25	Coronary artery imaging: 3D segmented k-space data acquisition with multiple breath-holds and real-time slab following. Journal of Magnetic Resonance Imaging, 2001, 13, 301-307.	3.4	35
26	Resting myocardial perfusion quantification with CMR arterial spin labeling at 1.5 T and 3.0 T. Journal of Cardiovascular Magnetic Resonance, 2008, 10, 53.	3.3	34
27	Noncontrast skeletal muscle oximetry. Magnetic Resonance in Medicine, 2014, 71, 318-325.	3.0	34
28	Endogenous contrast T1rho cardiac magnetic resonance for myocardial fibrosis in hypertrophic cardiomyopathy patients. Journal of Cardiology, 2015, 66, 520-526.	1.9	34
29	Efficacy of slow infusion of gadolinium contrast agent in three-dimensional MR coronary artery imaging. Journal of Magnetic Resonance Imaging, 1999, 10, 800-805.	3.4	33
30	Quantify patient-specific coronary material property and its impact on stress/strain calculations using in vivo IVUS data and 3D FSI models: a pilot study. Biomechanics and Modeling in Mechanobiology, 2017, 16, 333-344.	2.8	33
31	Quantification of Regional Myocardial Oxygenation by Magnetic Resonance Imaging. Circulation: Cardiovascular Imaging, 2010, 3, 41-46.	2.6	32
32	Myocardial Blood Volume Is Associated With Myocardial Oxygen Consumption. JACC: Cardiovascular Imaging, 2009, 2, 1313-1320.	5.3	31
33	Coronary artery imaging using contrast-enhanced 3D segmented EPI. Journal of Magnetic Resonance Imaging, 2001, 13, 676-681.	3.4	28
34	Quantitative assessment of coronary artery plaque vulnerability by high-resolution magnetic resonance imaging and computational biomechanics: A pilot study ex vivo. Magnetic Resonance in Medicine, 2005, 54, 1360-1368.	3.0	28
35	Quantification of Myocardial Blood Volume During Dipyridamole and Doubtamine Stress: A Perfusion CMR Study. Journal of Cardiovascular Magnetic Resonance, 2007, 9, 785-792.	3.3	28
36	Cap inflammation leads to higher plaque cap strain and lower cap stress: An MRI-PET/CT-based FSI modeling approach. Journal of Biomechanics, 2017, 50, 121-129.	2.1	28

#	Article	IF	CITATIONS
37	CCR2 Positron Emission Tomography for the Assessment of Abdominal Aortic Aneurysm Inflammation and Rupture Prediction. Circulation: Cardiovascular Imaging, 2020, 13, e009889.	2.6	28
38	Morphological and Stress Vulnerability Indices for Human Coronary Plaques and Their Correlations with Cap Thickness and Lipid Percent: An IVUS-Based Fluid-Structure Interaction Multi-patient Study. PLoS Computational Biology, 2015, 11, e1004652.	3.2	28
39	Accuracy of T1 measurements at high temporal resolution: Feasibility of dynamic measurement of blood T1 after contrast administration. Journal of Magnetic Resonance Imaging, 1999, 10, 576-581.	3.4	27
40	Dynamic estimation of the myocardial oxygen extraction ratio during dipyridamole stress by MRI: A preliminary study in canines. Magnetic Resonance in Medicine, 2004, 51, 718-726.	3.0	27
41	Vitamin D Levels Are Unrelated to the Severity of Respiratory Syncytial Virus Bronchiolitis Among Hospitalized Infants. Journal of the Pediatric Infectious Diseases Society, 2015, 4, 182-188.	1.3	27
42	Roles of myocardial blood volume and flow in coronary artery disease: an experimental MRI study at rest and during hyperemia. European Radiology, 2010, 20, 2005-2012.	4.5	26
43	A pilot study of regional perfusion and oxygenation in calf muscles of individuals with diabetes with a noninvasive measure. Journal of Vascular Surgery, 2014, 59, 419-426.	1.1	26
44	Combining IVUS and Optical Coherence Tomography for More Accurate Coronary Cap Thickness Quantification and Stress/Strain Calculations: A Patient-Specific Three-Dimensional Fluid-Structure Interaction Modeling Approach. Journal of Biomechanical Engineering, 2018, 140, .	1.3	26
45	Targeted Contrast Agent Helps to Monitor Advanced Plaque During Progression: A Magnetic Resonance Imaging Study in Rabbits. Investigative Radiology, 2008, 43, 49-55.	6.2	25
46	Three-dimensional MR pulmonary perfusion imaging and angiography with an injection of a new blood pool contrast agent B-22956/1. Journal of Magnetic Resonance Imaging, 2001, 14, 425-432.	3.4	23
47	Feasibility study of myocardial perfusion and oxygenation by noncontrast MRI: comparison with PET study in a canine model. Magnetic Resonance Imaging, 2008, 26, 11-19.	1.8	22
48	Accurate Measurement of Small Airways on Low-Dose Thoracic CT Scans in Smokers. Chest, 2013, 143, 1321-1329.	0.8	22
49	Blood-Brain Barrier Disruption and Perivascular Beta-Amyloid Accumulation in the Brain of Aged Rats with Spontaneous Hypertension: Evaluation with Dynamic Contrast-Enhanced Magnetic Resonance Imaging. Korean Journal of Radiology, 2018, 19, 498.	3.4	22
50	MR extracellular volume mapping and non-contrast T1ï•mapping allow early detection of myocardial fibrosis in diabetic monkeys. European Radiology, 2019, 29, 3006-3016.	4.5	22
51	Improvement of quantification of myocardial first-pass perfusion mapping: A temporal and spatial wavelet denoising method. Magnetic Resonance in Medicine, 2006, 56, 439-445.	3.0	21
52	Cardiac <sup>17</sup> 0 MRI: Toward direct quantification of myocardial oxygen consumption. Magnetic Resonance in Medicine, 2010, 63, 1442-1447.	3.0	21
53	3D MRI-based multicomponent thin layer structure only plaque models for atherosclerotic plaques. Journal of Biomechanics, 2016, 49, 2726-2733.	2.1	20
54	Altered Left Ventricular Geometry Changes the Border Zone Temporal Distribution of Stress in an Experimental Model of Left Ventricular Aneurysm: A Finite Element Model Study. Circulation, 2002, 106, .	1.6	20

#	Article	IF	CITATIONS
55	Relationship of apparent myocardial T2 and oxygenation: Towards quantification of myocardial oxygen extraction fraction. Journal of Magnetic Resonance Imaging, 2004, 20, 233-241.	3.4	19
56	Fluid-structure interaction models based on patient-specific IVUS at baseline and follow-up for prediction of coronary plaque progression by morphological and biomechanical factors: A preliminary study. Journal of Biomechanics, 2018, 68, 43-50.	2.1	19
57	Intravenous contrastâ€free standardized exercise perfusion imaging in diabetic feet with ulcers. Journal of Magnetic Resonance Imaging, 2019, 50, 474-480.	3.4	19
58	Single-Session Magnetic Resonance Coronary Angiography and Myocardial Perfusion Imaging Using the New Blood Pool Compound B-22956 (Gadocoletic Acid). Investigative Radiology, 2005, 40, 604-613.	6.2	17
59	A non-contrast CMR index for assessing myocardial fibrosis. Magnetic Resonance Imaging, 2017, 42, 69-73.	1.8	17
60	Stiffness Properties of Adventitia, Media, and Full Thickness Human Atherosclerotic Carotid Arteries in the Axial and Circumferential Directions. Journal of Biomechanical Engineering, 2017, 139, .	1.3	17
61	Contrast-enhanced coronary MR angiography: Relationship between coronary artery delineation and blood T1. Journal of Magnetic Resonance Imaging, 2001, 14, 348-354.	3.4	15
62	Cardiac Applications of PET/MR Imaging. Magnetic Resonance Imaging Clinics of North America, 2017, 25, 325-333.	1.1	15
63	Use of low-dose computed tomography to assess pulmonary tuberculosis among healthcare workers in a tuberculosis hospital. Infectious Diseases of Poverty, 2017, 6, 68.	3.7	15
64	A Machine Learning-Based Method for Intracoronary OCT Segmentation and Vulnerable Coronary Plaque Cap Thickness Quantification. International Journal of Computational Methods, 2019, 16, 1842008.	1.3	15
65	Assessment of myocardial oxygen extraction fraction and perfusion reserve with BOLD imaging in a canine model with coronary artery stenosis. Journal of Magnetic Resonance Imaging, 2007, 26, 72-79.	3.4	14
66	Quantification of global myocardial oxygenation in humans: initial experience. Journal of Cardiovascular Magnetic Resonance, 2010, 12, 34.	3.3	14
67	Higher critical plaque wall stress in patients who died of coronary artery disease compared with those who died of other causes: A 3D FSI study based on ex vivo MRI of coronary plaques. Journal of Biomechanics, 2014, 47, 432-437.	2.1	14
68	Year 1 of the Bundled Payments for Care Improvement–Advanced Model. New England Journal of Medicine, 2021, 385, 618-627.	27.0	14
69	Feasibility of combining MR perfusion, angiography, and 3He ventilation imaging for evaluation of lung function in a porcine model1. Academic Radiology, 2005, 12, 202-209.	2.5	13
70	Moyamoya Phenomenon Secondary to Intracranial Atherosclerotic Disease: Diagnosis by 3T Magnetic Resonance Imaging. Journal of Neuroimaging, 2009, 19, 381-384.	2.0	13
71	Non-contrast MRI perfusion angiosome in diabetic feet. European Radiology, 2015, 25, 99-105.	4.5	13
72	<sup>64</sup> Cu-ATSM Positron Emission Tomography/Magnetic Resonance Imaging of Hypoxia in Human Atherosclerosis. Circulation: Cardiovascular Imaging, 2020, 13, e009791.	2.6	13

#	Article	IF	CITATIONS
73	In Hypertrophic Cardiomyopathy Reduction of Relative Resting Myocardial Blood Flow Is Related to Late Enhancement, T2-Signal and LV Wall Thickness. PLoS ONE, 2012, 7, e41974.	2.5	12
74	Using Optical Coherence Tomography and Intravascular Ultrasound Imaging to Quantify Coronary Plaque Cap Stress/Strain and Progression: A Follow-Up Study Using 3D Thin-Layer Models. Frontiers in Bioengineering and Biotechnology, 2021, 9, 713525.	4.1	11
75	A Multimodality Image-Based Fluid–Structure Interaction Modeling Approach for Prediction of Coronary Plaque Progression Using IVUS and Optical Coherence Tomography Data With Follow-Up. Journal of Biomechanical Engineering, 2019, 141, .	1.3	10
76	Using optical coherence tomography and intravascular ultrasound imaging to quantify coronary plaque cap thickness and vulnerability: a pilot study. BioMedical Engineering OnLine, 2020, 19, 90.	2.7	10
77	Predicting plaque vulnerability change using intravascular ultrasound + optical coherence tomography image-based fluid–structure interaction models and machine learning methods with patient follow-up data: a feasibility study. BioMedical Engineering OnLine, 2021, 20, 34.	2.7	10
78	Pooled Sequencing of Candidate Genes Implicates Rare Variants in the Development of Asthma Following Severe RSV Bronchiolitis in Infancy. PLoS ONE, 2015, 10, e0142649.	2.5	10
79	2D/3D CMR tissue tracking versus CMR tagging in the assessment of spontaneous T2DM rhesus monkeys with isolated diastolic dysfunction. BMC Medical Imaging, 2018, 18, 47.	2.7	9
80	Multi-factor decision-making strategy for better coronary plaque burden increase prediction: a patient-specific 3D FSI study using IVUS follow-up data. Biomechanics and Modeling in Mechanobiology, 2019, 18, 1269-1280.	2.8	9
81	Diffusion Tensor Imaging of the Calf Muscles in Subjects With and Without Diabetes Mellitus. Journal of Magnetic Resonance Imaging, 2019, 49, 1285-1295.	3.4	9
82	MRI-based biomechanical imaging: initial study on early plaque progression and vessel remodeling. Magnetic Resonance Imaging, 2009, 27, 1309-1318.	1.8	8
83	Assessment of myocardial edema and area at risk in a rat model of myocardial infarction with a faster T2 mapping method. Acta Radiologica, 2015, 56, 1085-1090.	1.1	8
84	<i>T</i> <sub>2</sub> mapping at 7T MRI can quantitatively assess intramyocardial hemorrhage in rats with acute reperfused myocardial infarction in vivo. Journal of Magnetic Resonance Imaging, 2016, 44, 194-203.	3.4	8
85	Effects of Residual Stress, Axial Stretch, and Circumferential Shrinkage on Coronary Plaque Stress and Strain Calculations: A Modeling Study Using IVUS-Based Near-Idealized Geometries. Journal of Biomechanical Engineering, 2017, 139, .	1.3	8
86	Cardiac Positron Emission Tomography-Magnetic Resonance Imaging. Journal of Thoracic Imaging, 2018, 33, 139-146.	1.5	8
87	Self-Gated Late Gadolinium Enhancement at 7T to Image Rats with Reperfused Acute Myocardial Infarction. Korean Journal of Radiology, 2018, 19, 247.	3.4	8
88	Using intravascular ultrasound image-based fluid-structure interaction models and machine learning methods to predict human coronary plaque vulnerability change. Computer Methods in Biomechanics and Biomedical Engineering, 2020, 23, 1267-1276.	1.6	8
89	Noncontrast T1ï•dispersion imaging is sensitive to diffuse fibrosis: A cardiovascular magnetic resonance study at 3T in hypertrophic cardiomyopathy. Magnetic Resonance Imaging, 2022, 91, 1-8.	1.8	8
90	Oximetric angiosome imaging in diabetic feet. Journal of Magnetic Resonance Imaging, 2016, 44, 940-946.	3.4	7

#	Article	IF	CITATIONS
91	Human Recombinant Apyrase Therapy Protects Against Myocardial Ischemia/Reperfusion Injury and Preserves Left Ventricular Systolic Function in Rats, as Evaluated by 7T Cardiovascular Magnetic Resonance Imaging. Korean Journal of Radiology, 2020, 21, 647.	3.4	7
92	Injectable, thermosensitive, fast gelation, bioeliminable, and oxygen sensitive hydrogels. Materials Science and Engineering C, 2019, 99, 1191-1198.	7.3	6
93	Deteriorated regional calf microcirculation measured by contrast-free MRI in patients with diabetes mellitus and relation with physical activity. Diabetes and Vascular Disease Research, 2021, 18, 147916412110290.	2.0	6
94	Image-based biomechanical modeling for coronary atherosclerotic plaque progression and vulnerability prediction. International Journal of Cardiology, 2022, 352, 1-8.	1.7	6
95	Multi-patient study for coronary vulnerable plaque model comparisons: 2D/3D and fluid–structure interaction simulations. Biomechanics and Modeling in Mechanobiology, 2021, 20, 1383-1397.	2.8	4
96	Synthesis of Biomimetic Melanin-Like Multifunctional Nanoparticles for pH Responsive Magnetic Resonance Imaging and Photothermal Therapy. Nanomaterials, 2021, 11, 2107.	4.1	4
97	Disease-specific cardiovascular positron emission tomography/magnetic resonance imaging: a brief review of the current literature. Quantitative Imaging in Medicine and Surgery, 2016, 6, 297-307.	2.0	3
98	Evaluation of the Differences of Myocardial Fibers between Acute and Chronic Myocardial Infarction: Application of Diffusion Tensor Magnetic Resonance Imaging in a Rhesus Monkey Model. Korean Journal of Radiology, 2016, 17, 725.	3.4	3
99	Dynamic Diffusion Tensor Imaging Reveals Structural Changes in the Bilateral Pyramidal Tracts after Brain Stem Hemorrhage in Rats. Frontiers in Neuroanatomy, 2016, 10, 33.	1.7	3
100	In Vivo Intravascular Ultrasound-Based 3D Thin-Walled Model for Human Coronary Plaque Progression Study: Transforming Research to Potential Commercialization. International Journal of Computational Methods, 2019, 16, 1842011.	1.3	3
101	Evaluating the correlation of the impairment between skeletal muscle and heart using MRI in a spontaneous type 2 diabetes mellitus rhesus monkey model. Acta Diabetologica, 2020, 57, 673-679.	2.5	3
102	Microcirculation of intramyocardial hemorrhage caused by reperfused myocardial infarctions with ultrasmall superparamagnetic iron oxide cardiac magnetic resonance imaging. Acta Radiologica, 2022, 63, 1469-1474.	1.1	3
103	Compact <scp>MR</scp> â€compatible ergometer and its application in cardiac <scp>MR</scp> under exercise stress: A preliminary study. Magnetic Resonance in Medicine, 2022, 88, 1927-1936.	3.0	3
104	Improvement of hyperemic myocardial oxygen extraction fraction estimation by a diffusionâ€prepared sequence. Magnetic Resonance in Medicine, 2010, 63, 1675-1682.	3.0	2
105	Myocardial Hypoxia in Dilated Cardiomyopathy: Is it Just a Matter of Supply and Demand?. Circulation: Heart Failure, 2015, 8, 1011-1013.	3.9	2
106	Liver extracellular volume fraction values obtained with magnetic resonance imaging can quantitatively stage liver fibrosis: a validation study in monkeys with nonalcoholic steatohepatitis. European Radiology, 2020, 30, 5748-5757.	4.5	2
107	Quantification of myocardial oxygen extraction fraction: A proofâ€ofâ€concept study. Magnetic Resonance in Medicine, 2021, 85, 3318-3325.	3.0	2
108	Pilot study of contrast-free MRI reveals significantly impaired calf skeletal muscle perfusion in diabetes with incompressible peripheral arteries. Vascular Medicine, 2021, 26, 367-373.	1.5	2

#	Article	IF	CITATIONS
109	T <sub>2</sub> preparation method for measuring hyperemic myocardial O <sub>2</sub> consumption: in vivo validation by positron emission tomography. Journal of Magnetic Resonance Imaging, 2011, 33, 320-327.	3.4	1
110	Assessment of myocardial oxygenation with MRI. Quantitative Imaging in Medicine and Surgery, 2013, 3, 67-72.	2.0	1
111	Prognosis in patients with coronary heart disease and breath-holding limitations: a free-breathing cardiac magnetic resonance protocol at 3.0ÂT. BMC Cardiovascular Disorders, 2021, 21, 580.	1.7	1
112	Analysis of Stable Chelate-free Gadolinium Loaded Titanium Dioxide Nanoparticles for MRI-Guided Radionuclide Stimulated Cancer Treatment. Current Analytical Chemistry, 2022, 18, 826-835.	1.2	1
113	111 Detection of changes in myocardial blood flow and volume: a CMR study in a canine model of coronary artery stenosis. Journal of Cardiovascular Magnetic Resonance, 2008, 10, .	3.3	0
114	1090 Black-blood myocardial T2 and oxygenation imaging using a diffusion-weighted prepared sequence. Journal of Cardiovascular Magnetic Resonance, 2008, 10, A215.	3.3	0
115	139 Determination of myocardial OEF with a CMR method in a stenotic dog study. Journal of Cardiovascular Magnetic Resonance, 2008, 10, A40.	3.3	0
116	231 Alternation of myocardial oxygen consumption during hyperemia: detection with a CMR method. Journal of Cardiovascular Magnetic Resonance, 2008, 10, .	3.3	0
117	Myocardial Oxygenation Imaging: New Methods for Ischemia Detection. Current Cardiovascular Imaging Reports, 2011, 4, 159-164.	0.6	0
118	Oximetric angiosome imaging in diabetic feet. Journal of Magnetic Resonance Imaging, 2016, 44, spcone-spcone.	3.4	0
119	Negative Correlation of Wall Thickness With Wall Blood Pressure in a Patient-Specific Atherosclerotic Coronary Artery: A Case Report. , 2012, , .		0
120	Abstract 379: Introducing Stress-Based Quantitative Plaque Vulnerability Index for Patients with Coronary Artery Disease. Arteriosclerosis, Thrombosis, and Vascular Biology, 2015, 35, .	2.4	0
121	Abstract 646: A Simple Multi-Risk-Factor Decision-Making Strategy for Improved Coronary Plaque Burden Increase Prediction: a Patient-Specific 3D FSI Study Using IVUS Follow-up. Arteriosclerosis, Thrombosis, and Vascular Biology, 2018, 38, .	2.4	0
122	Low-dose dobutamine cardiovascular magnetic resonance segmental strain study of early phase of intramyocardial hemorrhage rats. BMC Medical Imaging, 2021, 21, 173.	2.7	0